Reflected wave of finite circulation from magnetic photonic crystals

2010 J. Phys.: Condens. Matter 22 182201

(http://iopscience.iop.org/0953-8984/22/18/182201)

IOP FTC
IOP PUBLISHING JOURNAL OF PHYSICS: CONDENSED MATTER
J. Phys.: Condens. Matter **22** (2010) 182201 (4pp) doi:10.1088/0953-8984/22/18/182201

FAST TRACK COMMUNICATION

Reflected wave of finite circulation from magnetic photonic crystals

S T Chui[1], **Shiyang Liu**[1,2] **and Zhifang Lin**[1,2]

[1] Bartol Research Institute, University of Delaware, Newark, DE 19716, USA
[2] Surface Physics Laboratory, Department of Physics, Fudan University, Shanghai 200433, People's Republic of China

Received 22 December 2009, in final form 2 March 2010
Published 15 April 2010
Online at stacks.iop.org/JPhysCM/22/182201

Abstract
We study the reflection of electromagnetic waves from a two-dimensional magnetic photonic crystal consisting of a periodic array of magnetic cylinders. At some frequencies the reflected wave is found to exhibit a strong circulation in that, locally, the angular momenta of the components are all of the same sign. As a result of this finite circulation, beams incident from different directions exhibit a dramatic change in their reflected waves. This effect can be used to build subwavelength one way waveguides, nearly perfect beam benders and splitters.

(Some figures in this article are in colour only in the electronic version)

Magnetic materials are irreplaceable ingredients in non-reciprocal 'one way' optical devices such as isolators and circulators [1]. Because of recent interest in meta-materials there has been a revival in activity exploring novel optical properties of systems with magnetic components [2]. These studies exploit asymmetries in the photonic dispersion between the forward and the backward directions that become possible in systems without inversion symmetry. In magnetic systems with inversion symmetry, even though the dispersion is symmetric, the wavefunctions for opposite propagating directions can become asymmetric. In this paper we examine an example of this wavefunction asymmetry and its physical consequences.

A plane wave can be considered as a linear combination of waves with different angular momenta. For example, in two dimensions a plane wave of wavevector $\boldsymbol{k}$ can be expanded in terms of Bessel functions $J_m(kr)$ as a sum of states of different angular momenta: $\exp(\mathrm{i}\boldsymbol{k}\cdot\boldsymbol{r}) = \sum_m \mathrm{i}^m \exp[\mathrm{i}m(\phi - \phi_k)]J_m(kr)$, where (r, ϕ) are the spatial cylindrical coordinates. There are equal amounts of angular momenta components of opposite signs $\pm m$. We find that, when a plane electromagnetic (EM) wave is incident on a magnetic photonic crystal (MPC) consisting of a periodic array of magnetic cylinders, at some frequencies the reflected wave from a cylinder consists mostly of angular momenta of the same sign. For example, the *local* reflected wave can be well approximated by

$$-b_0 H_0(kr) - \mathrm{i}b_1 \exp(\mathrm{i}\phi) H_1(kr) \tag{1}$$

where b_0, b_1 are amplitudes for the $m = 0$ and the $m = 1$ components. The components with negative m are very small. The reflected wave develops a 'finite circulation'. This 'finite circulation' exhibits dramatic physical manifestations. For beams incident from different directions on the same surface a dramatic change for the reflected waves is exhibited. This effect can be exploited to construct one way subwavelength waveguides that exhibit a superflow behavior, as well as nearly perfect beam benders and splitters [4]. We now describe our results in detail.

Our numerical calculation is carried out with the rigorous multiple scattering theory [5]. To clarify the physics we develop a simple controlled analytic approximation and compare this with exact full-wave numerical calculations. In the multiple scattering theory the scattered field from a site i, $\boldsymbol{b}_i$, is related to the total incoming field $\boldsymbol{f}_i$ by the scattering matrix of a single cylinder, t, in the form $\boldsymbol{b}_i = t\boldsymbol{f}_i$. The m th component of the inverse single cylinder t matrix can be expressed in terms of the scattering phase shift η by $t_m^{-1} = 1 - \mathrm{i}\cot\eta_m$. The total incoming field is a sum of the external incoming field $\boldsymbol{p}_i$ and the scattered waves from all the other scatters of the MPC slab, which can be written as: $\boldsymbol{f}_i = [\sum_{j\neq i} -\boldsymbol{S}_{ij}\boldsymbol{b}_j + \boldsymbol{p}_i]$. Here $\boldsymbol{S}_{ij}$ is a 'structure factor' that

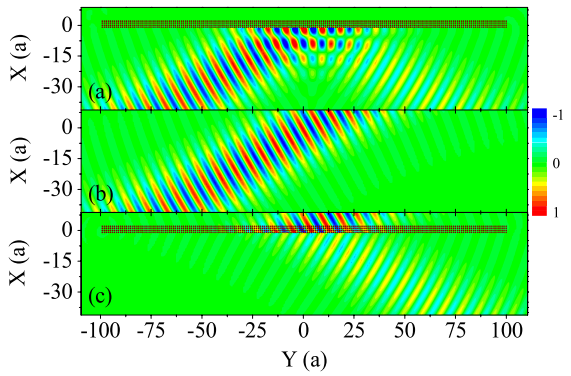

Figure 1. The electric field pattern of (a) the total field, (b) the incoming field, and (c) the scattered field for a Gaussian beam incident from left-hand side (incident angle $\theta_{\rm inc} = 60°$) upon a four-layer MPC slab. The electric field polarization of the Gaussian beam is along the cylinder axis. The position of the ferrite rods are marked by the black dot.

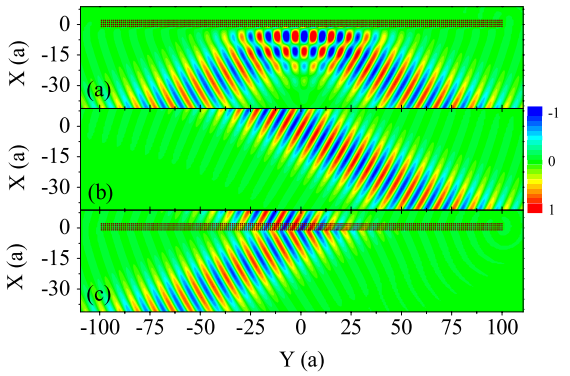

Figure 2. The electric field pattern of (a) the total field, (b) the incoming field, and (c) the scattered field for a Gaussian beam incident from right-hand side (incident angle $\theta_{\rm inc} = -60°$) upon a four-layer MPC slab. The electric field polarization of the Gaussian beam is along the cylinder axis. The position of the ferrite rods are marked by the black dot.

transforms the outgoing wave from site j into an incoming wave at site i. The scattering amplitude $\boldsymbol{b}$ from the MPC slab is related to the amplitude $\boldsymbol{p}_i$ of the external wave by the full $\boldsymbol{T}$ matrix: $\boldsymbol{b}_i = \boldsymbol{T}\boldsymbol{p}_i$. From the above reasoning, we find that the inverse $\boldsymbol{T}$ matrix of the MPC slab is a sum of the single cylinder inverse t matrix and the structure factor $\boldsymbol{S}$:

$$\boldsymbol{T}^{-1} = t^{-1} + \boldsymbol{S}. \tag{2}$$

The structure factor is determined from the geometry of the MPC slab and the scattering phase shift is determined from the susceptibilities of the cylinder. We next discuss the behavior of the phase shift and the operating frequency.

As a way to circumvent the diffraction limit for optical waveguides, surface plasmons (SP) have attracted much attention recently [9]. In the long wavelength limit, the p wave phase shift for the TE mode is given by $\tan\eta_{\pm 1} = \pi(kR/2)^2(\epsilon - 1)/(\epsilon + 1)$. A surface plasmon occurs when the dielectric constant ϵ is equal to -1 in two dimensions. The surface plasmon is thus manifested as a scattering resonance. Because of the symmetry of Maxwell's equations with respect to the magnetic and electric degrees of freedom, we expect a symmetric type of phenomena to occur when the effective magnetic susceptibility in 2D is equal to -1. Indeed, a scattering resonance occurs for the $m = +1$ TM mode when the effective magnetic susceptibility is equal to -1. We called this the magnetic surface plasmon (MSP) [7, 8]. For a periodic array of ferromagnets, coupled MSP *resonances* form *bulk* MSP bands [6, 8]. These MSP bands possess finite Chern numbers [10]. Our phenomenon comes from coupling to the bulk MSP states in the magnetic photonic crystal.

We have considered an example of a two-dimensional (2D) MPC composed of a square lattice (lattice constant $a = 8$ mm) of ferrite cylinders of radii $r = 0.25a$ in air. The axes of the cylinders and the magnetization M_0 are along the z direction. The permittivity of the ferrite rod is $\epsilon_s = 12.6 + \mathrm{i}7 \times 10^{-3}$. The magnetic susceptibility tensor is given by

$$\widehat{\mu} = \begin{bmatrix} \mu & -\mathrm{i}\mu' & 0 \\ \mathrm{i}\mu' & \mu & 0 \\ 0 & 0 & 1 \end{bmatrix}, \tag{3}$$

where μ, μ' is of a resonance form: $\mu = 1 + \omega_m(\omega_0 + \mathrm{i}\alpha\omega)/[(\omega_0 + \mathrm{i}\alpha\omega)^2 - \omega^2]$, $\mu' = \omega_m\omega/[(\omega_0 + \mathrm{i}\alpha\omega)^2 - \omega^2]$ with a spin wave resonance frequency $\omega_0 = \gamma H_0$, H_0 is a sum of the external field $H_{\rm ext}$ and the anisotropy field H_a. γ is the gyromagnetic ratio. $\omega_m = \gamma M_0$ measures the coupling strength of the magnetic material with the EM waves. For our calculation, we use $H_0 = 900$ Oe, $4\pi M_s = 1700$ Oe. The damping is controlled by a coefficient α, which we set equal to 7×10^{-3}. This is typical of the more readily available NiZn ferrites, but is twenty times larger than that for YIG, which was used recently in calculations of *edge state* one way waveguides [11]. In our numerical calculation, we have computed the matrix $\boldsymbol{T}$ by inverting the matrix $\boldsymbol{T}^{-1}$ for a finite four-layer MPC slab with each layer consisting of 200 ferrite rods. The scattering amplitudes are obtained by multiplying $\boldsymbol{T}$ and $\boldsymbol{p}$. In this paper we focus on polarizations with the electric (E mode) field parallel to the cylinder axis.

We have considered numerical examples of incoming Gaussian beams with angles of incidence of $\pm 60°$. The beam center is focused on the middle (100th) ferrite rod in the first layer. The working frequency is selected as $f_{\rm w} = 4.84$ GHz, located near to the MSP frequency $f_s = \frac{1}{2\pi}(\omega_0 + \frac{1}{2}\omega_m) = 4.9$ GHz.

In figures 1 and 2 we show the electric field of reflected Gaussian beams of EM waves coming in opposite y directions. In one direction, the reflected wave is very weak (figure 1) while in the other direction the intensity of the reflected wave remains substantial. It is evident that there exists a remarkable difference for reflected Gaussian beams in different directions[3].

[3] In [4] we found numerically that for a line source close to the surface, the reflection nearly disappears on one side of the source. This line source is coupled to *both* surface and bulk states. In the present calculation no surface state exists at the wavevectors of interest.

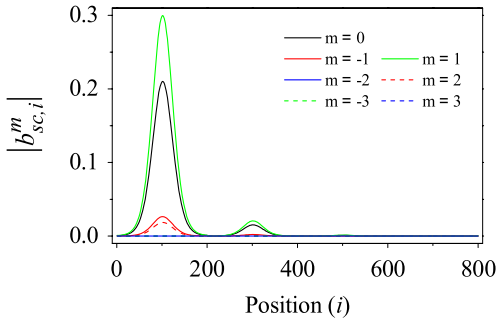

Figure 3. The scattering amplitude for different angular momenta components at different positions for an incoming angle of 60°. Labels 1–200, 201–400, 401–600, and 601–800 correspond to the first, second, third, and fourth layers.

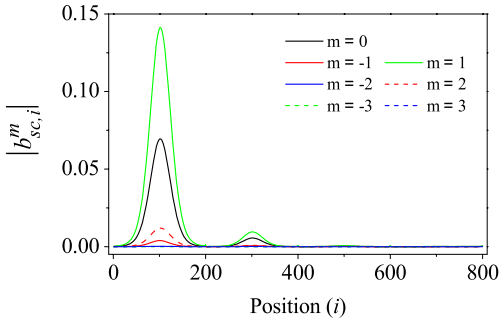

Figure 4. The scattering amplitude for different angular momenta components at different positions for an incoming angle of −60°. Labels 1–200, 201–400, 401–600, and 601–800 correspond to the first, second, third, and fourth layers.

Parallel to the surface there is reflection symmetry and the bulk photonic bands are the same for the two incoming directions. Our effect comes from the wavefunctions. To gain a deeper understanding of our results, we show the corresponding angular momenta components $|b_i^m|$ at the sites of different cylinders i of the MPC slab in figures 3 and 4. As shown, only angular momentum components of positive m (0 and 1) are dominant. There is a difference in magnitude for the opposite incoming directions. The scattering fields are only large in the first layer and do not penetrate into the MPC slab. This provides a simple way to obtain a controlled analytic approximation for the scattered fields.

As we mentioned, the total incoming field at a site i, $\boldsymbol{f}_i$, is the sum of the external incoming field $\boldsymbol{p}_i$ and the scattered waves from other scatterers of the MPC slab: $\boldsymbol{f}_i = \sum_{j\neq i} \boldsymbol{S}_{ij}\boldsymbol{b}_j + \boldsymbol{p}_i$. Because the scattered fields $\boldsymbol{b}_j$ are only significant in the first layer, in the sum over j we can restrict our attention to j terms only in the topmost first layer. The reflection problem for the 2D MPC can be well approximated by the reflection problem from a one-dimensional (1D) MPC consisting of the topmost layer. As usual, we consider an incoming plane wave so there is translational invariance along this layer. The eigenstates are characterized by a wavevector k_y. The 1D $\boldsymbol{T}$ matrix is diagonal in k_y, its inverse involves the coupling between angular momentum states and is given by $\boldsymbol{T}^{-1} = [t^{-1} + \boldsymbol{S}]$ with $\boldsymbol{S}(m) = \sum_{Y\neq 0} \exp(\mathrm{i}k_y Y) H_m(k_0 Y) \exp(\mathrm{i}m\phi_Y)$.

Near the MSP bands, only a few angular momentum states are important, and the inversion of T^{-1} is simple. More precisely, at this frequency range only a few scattering phase shifts are close to the resonance, so $\cot\eta_m$ is small. For most other m's $\cot\eta_m$ is large. Accordingly, $t_m^{-1} = 1 - \mathrm{i}\cot\eta_m$ is usually small only for a few positive m. The inversion of $\boldsymbol{T}^{-1}$ can be analytically carried out. For the example considered here, only the $m = 0$ and 1 phase shifts are significant. $\boldsymbol{T}^{-1}$ is then approximated by a 2×2 matrix, which can be easily inverted. More precisely, with $a_m = t_m^{-1} + \boldsymbol{S}(0)$ and $x = \boldsymbol{S}(1)$, we get

$$\boldsymbol{T} = \begin{bmatrix} a_1 & -x \\ x & a_0 \end{bmatrix} \Big/ (a_0 a_1 + x^2), \qquad \boldsymbol{p} = \begin{bmatrix} p_1 \\ p_0 \end{bmatrix}, \quad (4a)$$

$$\begin{bmatrix} b_1 \\ b_0 \end{bmatrix} = \begin{bmatrix} a_0 p_1 - x p_0 \\ a_1 p_0 + x p_1 \end{bmatrix} \Big/ \det, \quad (4b)$$

where $\det = (a_0 a_1 + x^2)$. Since $\exp(-\mathrm{i}\mathbf{k_i}\cdot\mathbf{r}) = \sum_n (-\mathrm{i})^n \exp[\mathrm{i}n(\phi - \phi_{ki})] J_n(k_i r)$, the incoming wave amplitude is given by $p_n = (-\mathrm{i})^n (k_{ix} - \mathrm{i}k_{iy})^n / k_i^n$.

The magnitude of angular momentum components of the scattered field obtained with equation (4) for a plane wave is shown in figure 5 as a function of the angle of incidence. This is in good agreement with our detailed numerical results, which are shown in figure 5 as well. We have performed calculations for incident plane waves and Gaussian beams. For the whole range of incidence angles, the results obtained for plane waves and Gaussian beam are almost the same. It can be seen that there exists a distinct asymmetry for the scattering amplitude of the positive and negative incident angles because of the finite circulation around the ferrite rods.

We next examine the physical meaning of the electric field in equation (1). The electric field at position $\boldsymbol{r}$ scattered from the collection of cylinders at positions $\boldsymbol{r}'_j$ is given by summing over the contributions from all the rods: $E = -\sum_j \mathrm{e}^{-\mathrm{i}k_y y'_j} [b_0 H_0(k_0 R) - b_1 H_1(k_0 R)(X + \mathrm{i}Y)/R]$, where $R = |\boldsymbol{r}'_j - \boldsymbol{r}|$, $X = x'_j - x$, and $Y = y'_j - y$. We focus on the far field when the sums can be replaced by integrals. When the sum of the wavelets from each cylinder is added up, the resulting reflected wave becomes

$$E \approx -2\exp(-\mathrm{i}k_x x - \mathrm{i}k_y y)[b_0 + \mathrm{i}b_1 \exp(\mathrm{i}\phi_k)]/|k_x|a, \quad (5)$$

where $\mathbf{k}$ is the wavevector and ϕ_k is its orientation. As the direction of $\mathbf{k}$ is varied, the sign of $\exp(\mathrm{i}\phi_k)$ can change. The s and the p wave contribution can switch between destructive and constructive interference. As a result the magnitude of the reflected beam is dramatically changed as the direction of k_x is reversed. This shows that the magnitude of the reflected wave depends on b_0, b_1 and ϕ_k, which in turn are functions of the incoming direction and thus depend on the sign of k_y, as is demonstrated in figures 1 and 2.

We have also considered the frequency dependence of our effect. As the frequency is increased, one moves away from the resonance; the $m = 1$ scattering phase shift is decreased. The $m = 0$ component becomes much bigger than the $m = 1$ component; the $m = 1$ component is almost the same as the

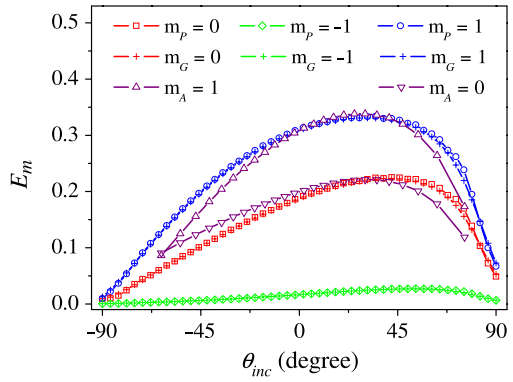

Figure 5. Numerical results for the magnitude of angular momentum components of the scattered field E_0, E_{-1}, and E_1 for plane waves (subscript P) and Gaussian beams (subscript G) as a function of the incidence angle (lines), and analytic results (subscript A) obtained with equation (5). The operating frequency is at $f = 4.8$ GHz.

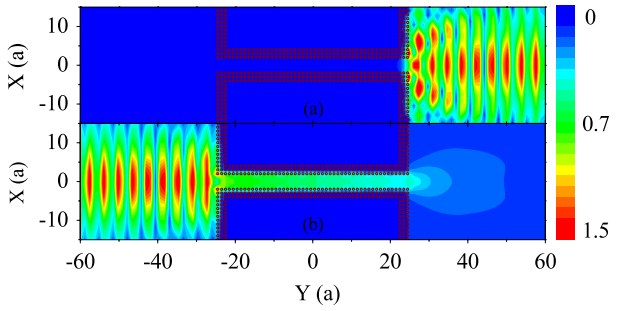

Figure 6. The electric field patterns when a Gaussian beam is incident along the channel with a width of the channel equal to $4a$. The Gaussian beam can pass the channel for one direction, while for the opposite direction it is completely suppressed.

$m = -1$ component. The circulation around the ferrite rod becomes small. The scattered amplitude for the positive and negative angle are almost the same. The scattering amplitude becomes nearly symmetric with respect to the incident angle.

Finally we demonstrate an application of our effect. A one way waveguide can be constructed from two MPCs of opposite magnetizations. In our guide, the EM wave is repeatedly one way reflected forward from the walls of the guide, similar to ideas in optical fibers. We have carried out a numerical demonstration of this effect. In figure 6 we show the electric field patterns when a Gaussian beam is incident along an interconnect/waveguide with a width of the channel equal to $4a$. There is an impedance mismatch, so the field inside is less than that outside. Once inside, the Gaussian beam can pass the channel for one direction, while for the opposite direction it is completely suppressed. One way waveguides have recently been proposed using 'edge' states localized near the surface [11]. Our guide does not rely on these localized states. The damping coefficient α in the present calculation is twenty times larger; the surface states become heavily damped. Furthermore the size of the surface states is less than a; the channel width here is larger than the combined size of the top and bottom surface states. One way electromagnetic Tamm states in magnetophotonic structures, due to an asymmetric dispersion, have also been discussed previously [3].

In conclusion we studied the reflection of EM waves from MPCs. The reflected wave is found to exhibit a strong circulation at some frequencies so that the scattering of some angular momentum states of one sign is close to the resonance condition. An example of this corresponds to the surface plasmon bands. Magnetic surface resonances also occur at frequencies close to the spin wave band [8] and we expect our calculation to be applicable to that case as well.

This work is partly supported by the DOE. ZFL is also supported by CNKBRSF, NNSFC, and SSTC (08dj1400302).

References

[1] For a recent perspective, see Chui S T 2008 Ferromagnetic metal–insulator multilayer radio frequency circulator *US Patent Specification* 7362195 B2
[2] Yu Z F, Wang Z and Fan S H 2007 *Appl. Phys. Lett.* **90** 121133
Takeda H and John S 2008 *Phys. Rev.* A **78** 15
Khanikaev A B and Steel M J 2009 *Opt. Express* **17** 5265–72
[3] Khanikaev A B, Baryshev A V, Inoue M and Kivshar Y S 2009 *Appl. Phys. Lett.* **95** 011101
[4] Liu S Y *et al* 2009 arXiv:0907.3127v1
See also Chui S T and Lin Z F 2007 *J. Phys.: Condens. Matter* **19** 406233
[5] Quinten M, Leitner A, Krenn J R and Aussenegg F R 1998 *Opt. Lett.* **23** 1331
[6] Chui S T and Lin Z F 2008 *Phys. Rev.* E **78** 065601(R)
[7] Damon R W and Eshbach J R 1961 *J. Phys. Chem. Solids* **19** 308
Hartstein A, Burstein E, Maradudin A A, Brewer R and Wallis R F 1973 *J. Phys. C: Solid State Phys.* **6** 1266
Gollub J R, Smith D R, Vier D C, Perram T and Mock J J 2005 *Phys. Rev.* B **71** 195402
[8] Liu S Y, Du J J, Lin Z F, Wu R X and Chui S T 2008 *Phys. Rev.* B **78** 155101
[9] Zayats A V, Smolyaninov I I and Maradudin A A 2005 *Phys. Rep.* **408** 131
Barnes W L, Dereux A and Ebbesen T W 2003 *Nature* **424** 824
Konopsky V N and Alieva E V 2006 *Phys. Rev. Lett.* **97** 253904
[10] Chui S T and Lin Z F 2009 unpublished
[11] Haldane F D M and Raghu S 2008 *Phys. Rev. Lett.* **100** 013904
Wang Z *et al* 2008 *Phys. Rev. Lett.* **100** 013905
Yu Z *et al* 2008 *Phys. Rev. Lett.* **100** 023902